Electrocatalytic, photocatalytic, fluorescence sensing and CO_2RR properties of a series of homopolymolybdate hybrid coordination polymers

Baoyue Zhang,[a] Jun Ying,[a,*] Xinyue Zhang,[a] Chen Wang[a], Aixiang Tian[a,*]

Table S1. Selected bond distances (Å) and angles (°) for coordination polymers **1–4**.

	1		
Cu(1)-O(1)#2	1.916(5)	Cu(1)-N(1)#2	1.914(8)
Cu(1)-O(1)	1.916(5)	Cu(1)-N(1)	1.914(8)
O(1)#2-Cu(1)-O(1)	180.00(18)	N(1)#2-Cu(1)-O(1)#2	87.0(3)
N(1)-Cu(1)-O(1)	87.0(3)	N(1)#2-Cu(1)-O(1)	93.0(3)
N(1)-Cu(1)-O(1)#2	93.0(3)	N(1)-Cu(1)-N(1)#2	180.0(5)
Mo(14)-O(1)-Cu(1)	139.0(3)	N(2)-N(1)-Cu(1)	119.6(5)
Symmetry codes for **1:** #1 -x+1,-y+1,-z+1		#2 -x+1,-y+1,-z+2	
	2		
Zn(1)-O(13)	2.135(4)	Zn(1)-O(14)#2	2.108(5)
Zn(1)-O(13)#2	2.135(4)	Zn(1)-N(1)	2.098(6)
Zn(1)-O(14)	2.108(5)	Zn(1)-N(1)#2	2.098(6)
O(13)-Zn(1)-O(13)#2	180.0	N(1)#2-Zn(1)-O(13)	82.67(16)
O(14)-Zn(1)-O(13)	93.45(17)	N(1)-Zn(1)-O(13)#2	82.67(16)
O(14)-Zn(1)-O(13)#2	86.55(17)	N(1)-Zn(1)-O(13)	97.33(16)
O(14)#2-Zn(1)-O(13)#2	93.46(17)	N(1)#2-Zn(1)-O(13)#2	97.33(16)
O(14)#2-Zn(1)-O(13)	86.54(17)	N(1)#2-Zn(1)-O(14)	86.6(2)
O(14)-Zn(1)-O(14)#2	180.0	N(1)#2-Zn(1)-O(14)#2	93.4(2)
Symmetry codes for **2:** #1 -x+1,-y+1,-z		#2 -x+1,-y+1,-z+1	
	3		
O(15)-Cu(1)	1.962(3)	O(17)-Cu(2)	1.974(3)
O(16)-Cu(1)	1.990(3)	O(14)-Cu(1)	1.939(3)
O(20)-Cu(2)	1.988(3)	O(18)-Cu(2)	1.938(3)
Cu(1)-N(1)	1.990(3)	Cu(2)-N(2)#2	2.320(3)
Cu(1)-N(3)	2.390(3)	Cu(2)-N(4)	2.007(3)
O(15)-Cu(1)-O(16)	94.55(14)	O(14)-Cu(1)-N(1)	81.66(12)
O(15)-Cu(1)-N(1)	93.95(13)	O(14)-Cu(1)-N(3)	92.30(12)

O(15)-Cu(1)-N(3)	93.45(12)	N(1)-Cu(1)-O(16)	164.71(13)
O(16)-Cu(1)-N(3)	88.23(11)	N(1)-Cu(1)-N(3)	103.92(11)
O(14)-Cu(1)-O(15)	173.47(12)	O(20)-Cu(2)-N(4)	160.64(12)
O(14)-Cu(1)-O(16)	88.72(13)	O(17)-Cu(2)-O(20)	95.94(12)

Symmetry codes for **3:** #1 -x+1,-y-2,-z #2 x-1,y,z #3 x+1,y,z

4

Cu(1)-O(3)	2.0603(15)	Cu(1)-O(4)#2	2.3249(15)
Cu(1)-O(6)	1.9742(15)	Cu(1)-N(1)	2.0001(19)
Cu(1)-O(5)#1	2.3036(15)	Cu(1)-N(2)	1.9761(19)
O(3)-Cu(1)-O(5)#1	75.43(6)	O(6)-Cu(1)-N(2)	92.32(7)
O(3)-Cu(1)-O(4)#2	74.39(6)	O(5)#1-Cu(1)-O(4)#2	147.09(6)
O(6)-Cu(1)-O(3)	89.32(6)	N(1)-Cu(1)-O(3)	96.97(7)
O(6)-Cu(1)-O(5)#1	83.84(6)	N(1)-Cu(1)-O(5)#1	101.82(7)
O(6)-Cu(1)-O(4)#2	83.00(6)	N(1)-Cu(1)-O(4)#2	94.56(7)
O(6)-Cu(1)-N(1)	172.41(7)	O(6)-Cu(1)-N(2)	92.32(7)
N(2)-Cu(1)-O(3)	178.17(7)	N(2)-Cu(1)-O(4)#2	106.60(7)
N(2)-Cu(1)-O(5)#1	103.95(7)	N(2)-Cu(1)-N(1)	81.45(8)

Symmetry codes for **4:** #1 x,-y+1/2,z+1/2 #2 x,-y+1/2,z-1/2

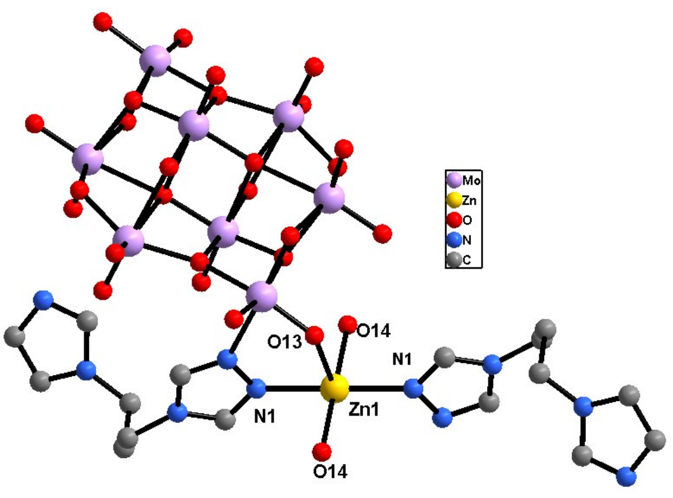

Fig. S1. Ball/stick diagram of the asymmetric unit of coordination polymer **2**. The hydrogen atoms are omitted for clarity.

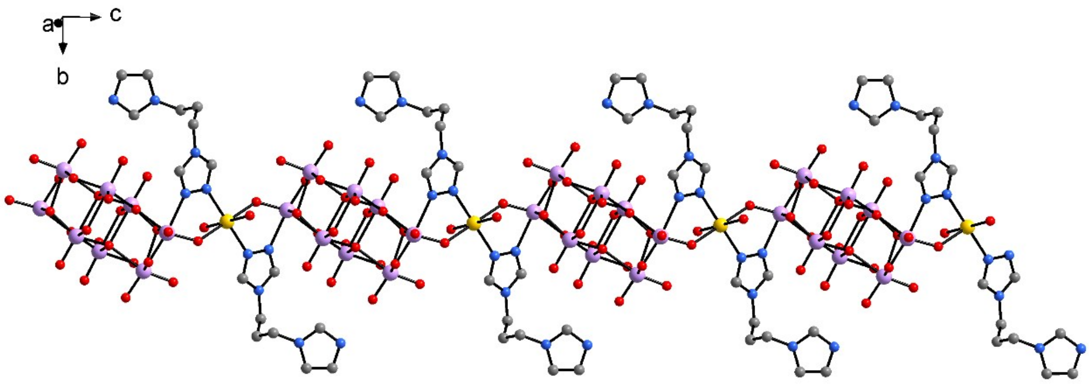

Fig. S2. The 1D chain of coordination polymer **2**.

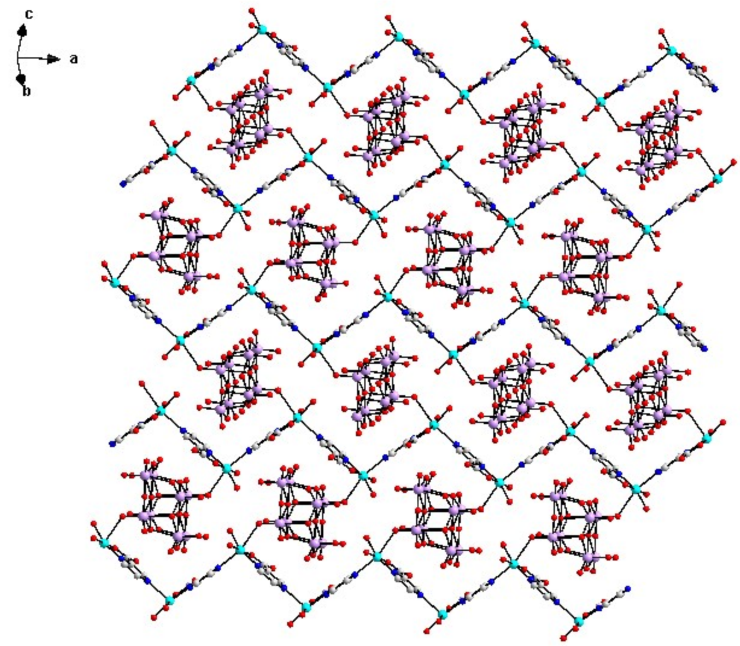

Fig. S3. The 2D layer of coordination polymer **3**.

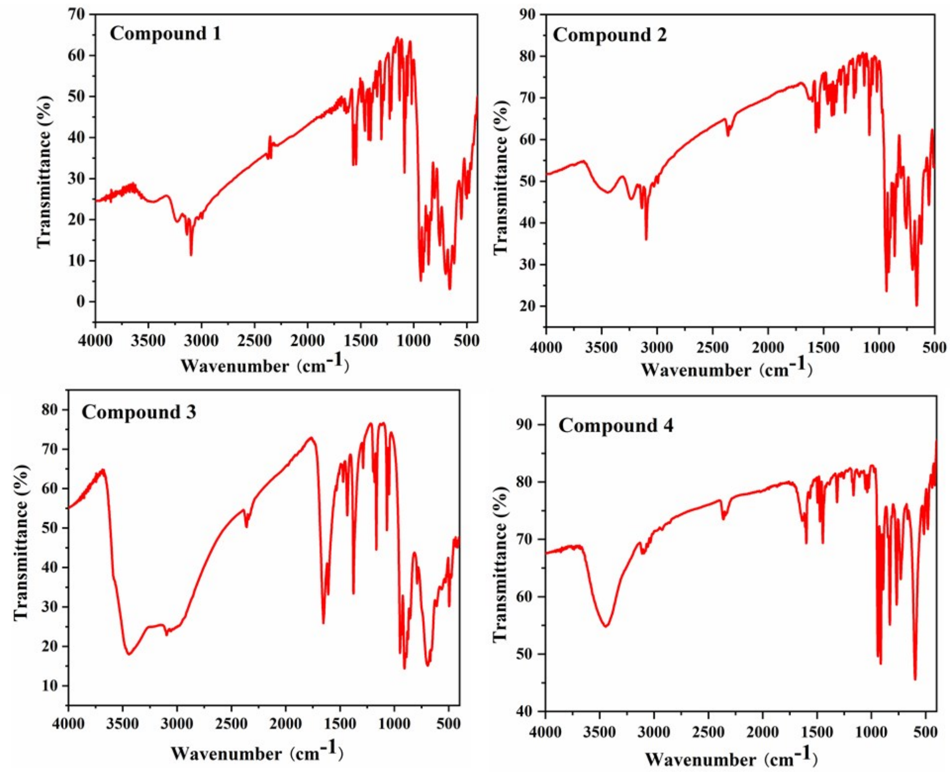

Fig. S4. The IR spectra of coordination polymers **1**−**4**.

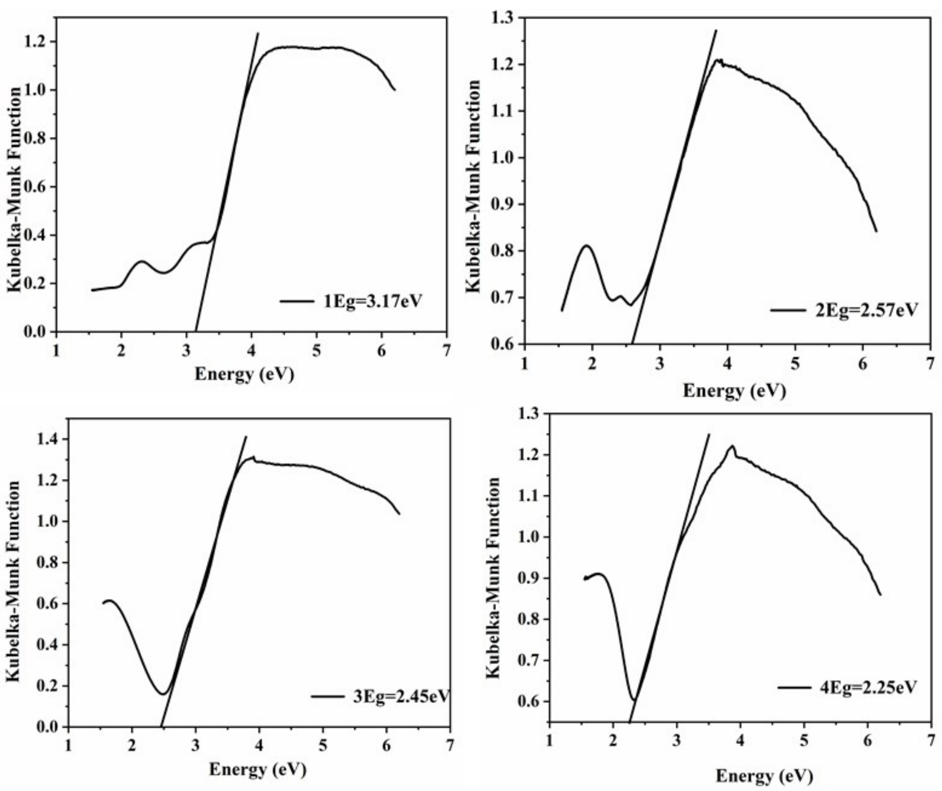

Fig. S5. Solid-state optical diffuse-reflection spectra of coordination polymers **1**−**4** derived from diffuse reflectance data at room temperature.

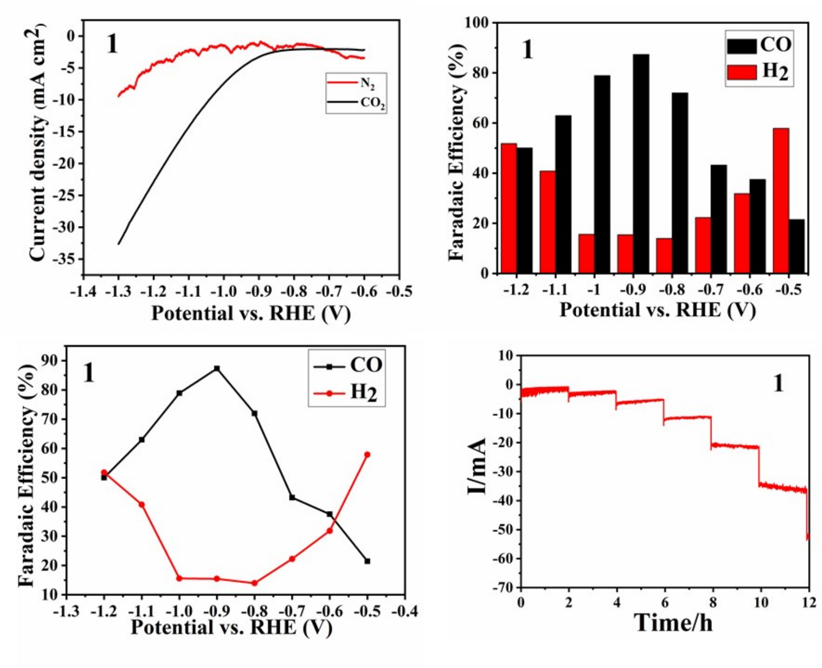

Fig. S6. (a) LSV curves of coordination polymer **1** in CO_2-saturated and N_2-saturated 0.5 M $KHCO_3$ electrolyte on carbon paper at a scan rate of 5 mV s^{-1}. (b) The FE of **1** for CO (red bars) and H_2 (black bars). (c) The FE of CO and H_2 products on **1** at selected potentials. (d) The i-t curve of **1** during the electrolysis.

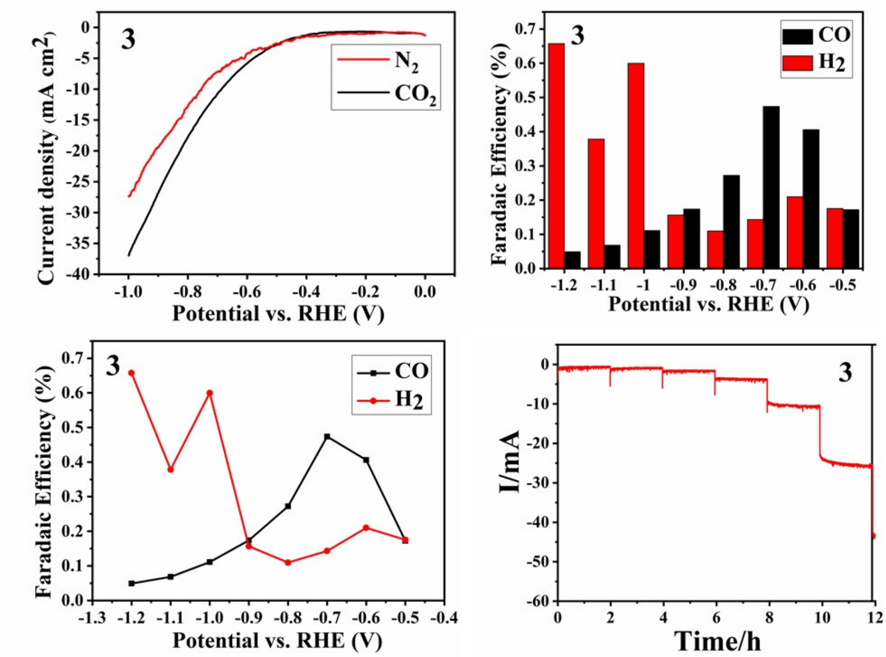

Fig. S7. (a) LSV curves of coordination polymer **3** in CO_2-saturated and N_2-saturated 0.5 M $KHCO_3$ electrolyte on carbon paper at a scan rate of 5 mV s^{-1}. (b) The FE of **3** for CO (red bars) and H_2 (black bars). (c) The FE of CO and H_2 products on **3** at selected potentials. (d) The i-t curve of **3** during the electrolysis.

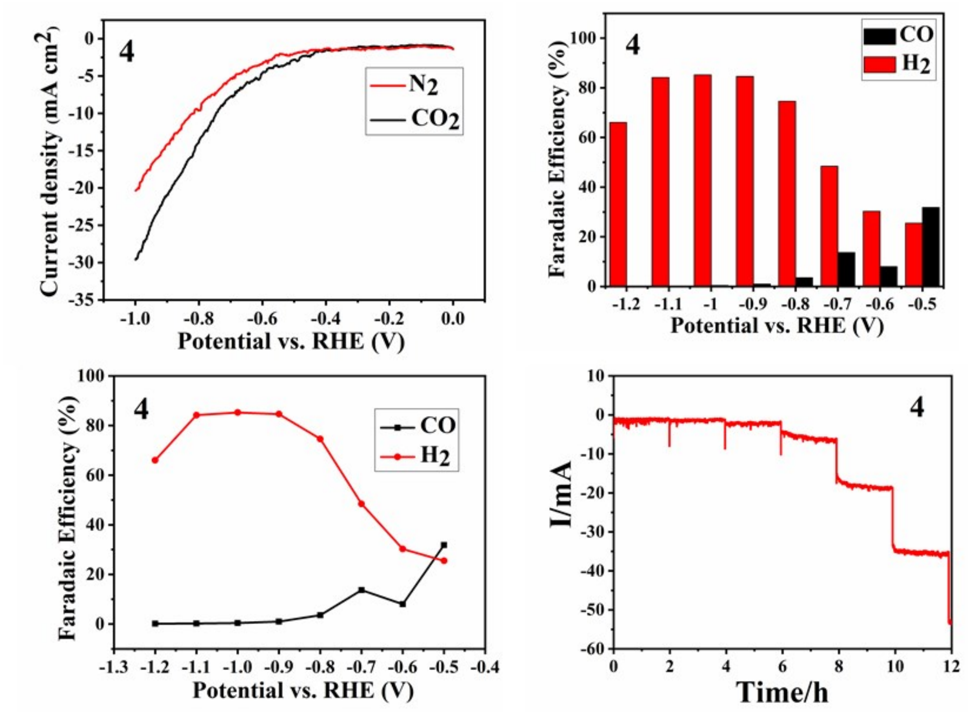

Fig. S8. (a) LSV curves of coordination polymer **4** in CO_2-saturated and N_2-saturated 0.5 M $KHCO_3$ electrolyte on carbon paper at a scan rate of 5 mV s^{-1}. (b) The FE of **4** for CO (red bars) and H_2 (black bars). (c) The FE of CO and H_2 products on **4** at selected potentials. (d) The i-t curve of **4** during the electrolysis.

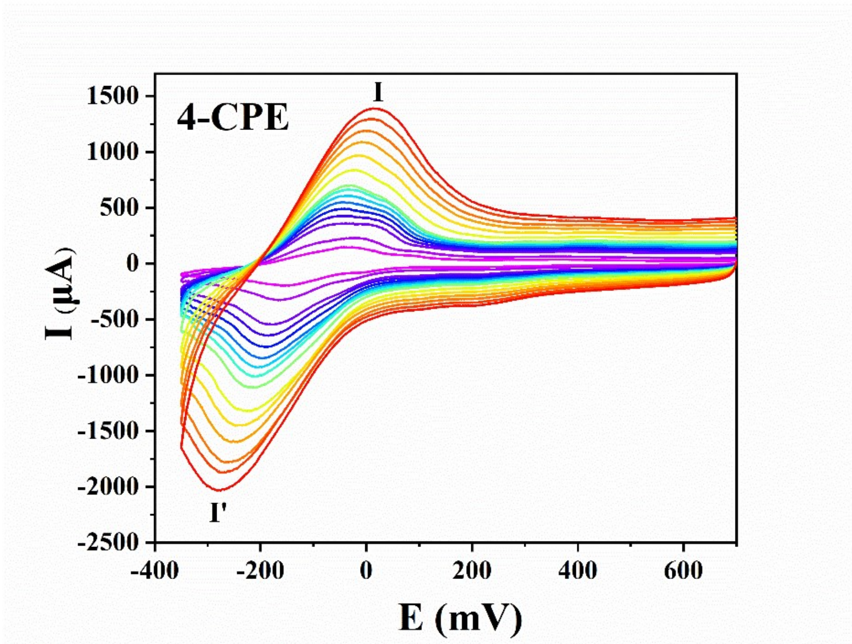

Fig. S9. The cyclic voltammograms of the **4**–CPEs in 0.1 M H_2SO_4 + 0.5 M Na_2SO_4 aqueous solution at different scan rates (from inner to outer: 20, 40, 60, 80, 100, 120, 140, 160, 180, 200, 250, 300, 350, 400, 450 and 500 mV·s^{-1}, respectively).

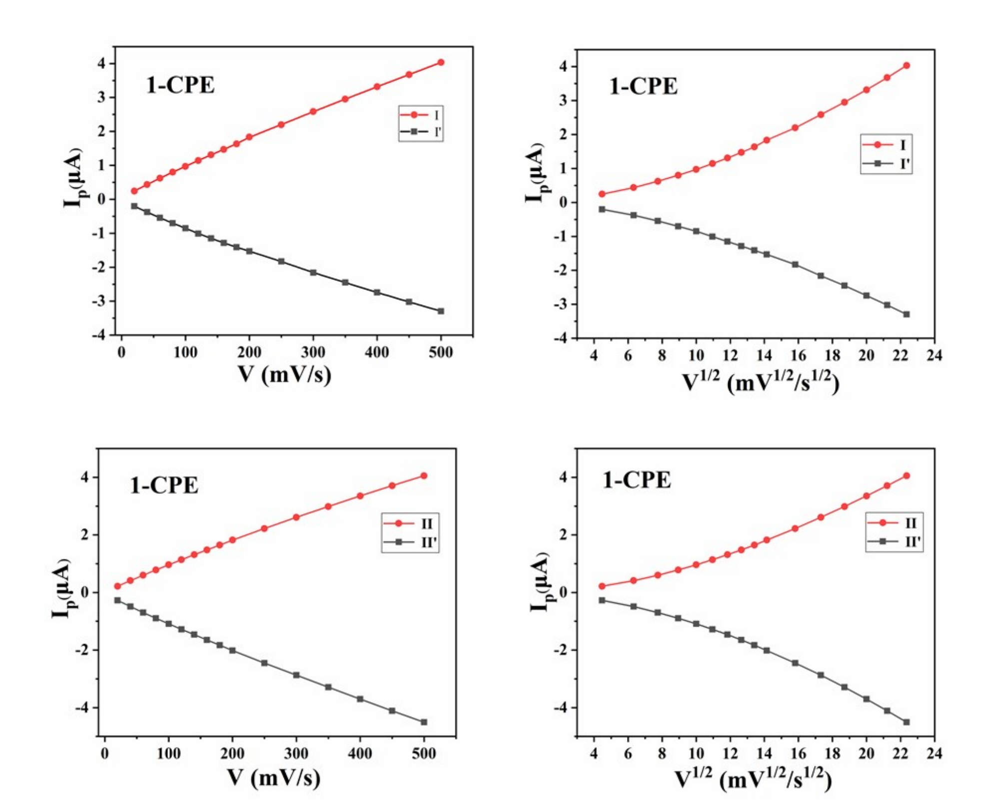

Fig. S10. Plots of the anodic and the cathodic peak I–I′ and II–II′ current against ν and $\nu^{1/2}$ of **1**–CPE.

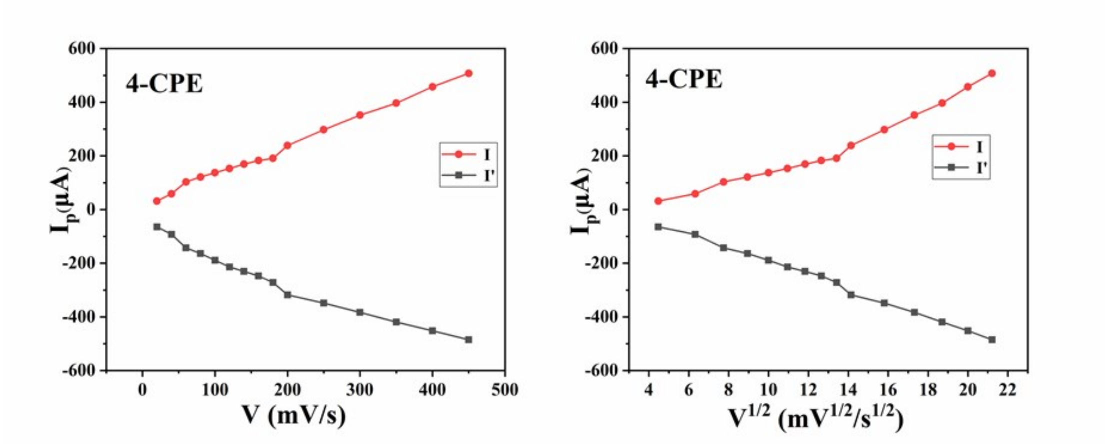

Fig. S11. Plots of the anodic and the cathodic peak I–I′current against ν and $\nu^{1/2}$ of **4**–CPE.

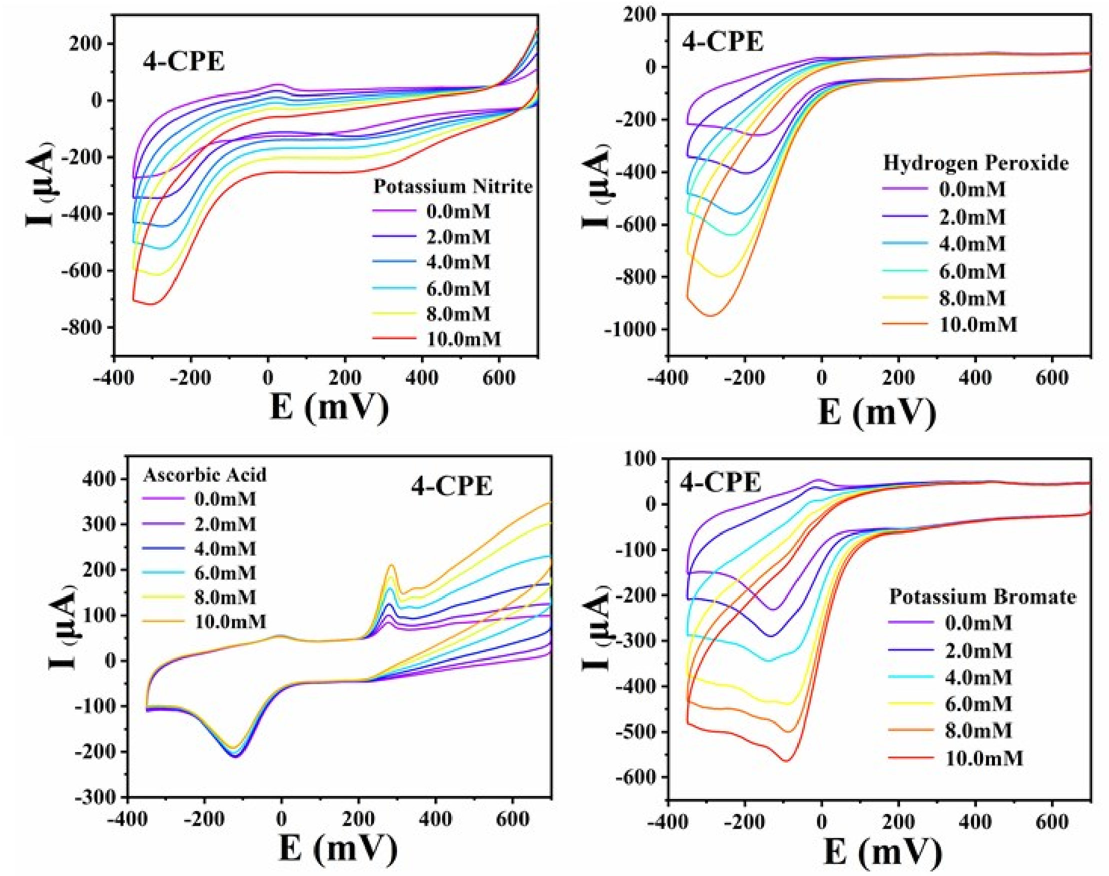

Fig. S12. Cyclic voltammograms of the **4**–CPE in 0.1 M H_2SO_4 + 0.5 M Na_2SO_4 aqueous solution containing0; 2; 4; 6; 8 and 10 mM KNO_2, H_2O_2, AA and $KBrO_3$. Scan rate: 250 mV·s^{-1}.

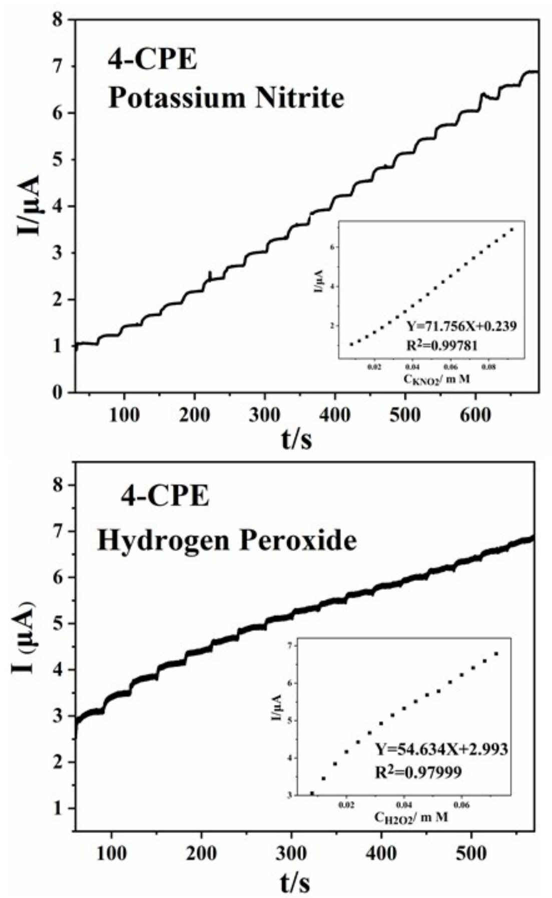

Fig. S13. Amperometric response for the **4**–CPEs on successive addition of 0.4 mM nitrite and H_2O_2 to 0.1 M H_2SO_4 + 0.5 M Na_2SO_4 aqueous solution. The inset: the steady-state calibration curve for current versus concentration (applied potential: -300 mV).

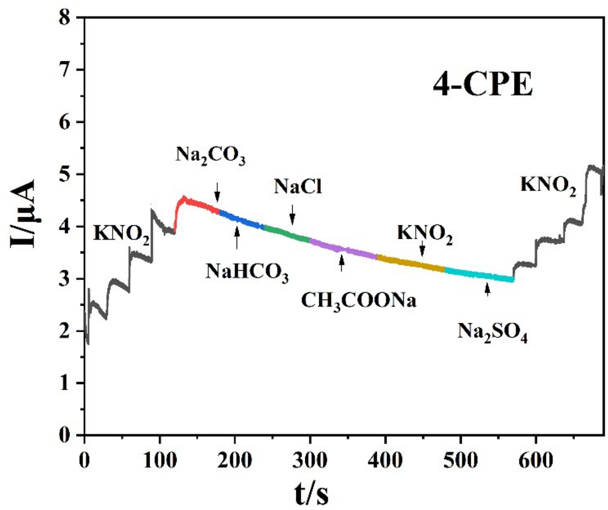

Fig. S14. Amperometric current responses of **4–**CPE in aqueous solution upon addition of various inorganic salts.

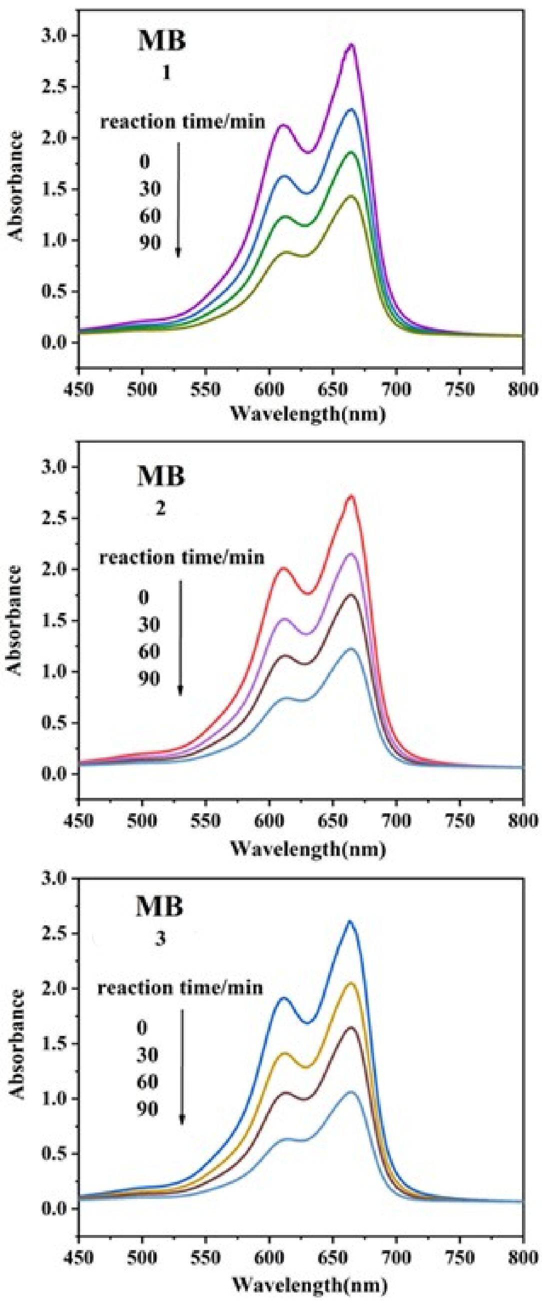

Fig. S15. Amperometric current responses of **1–3** CPE in aqueous solution upon addition of various inorganic salts.

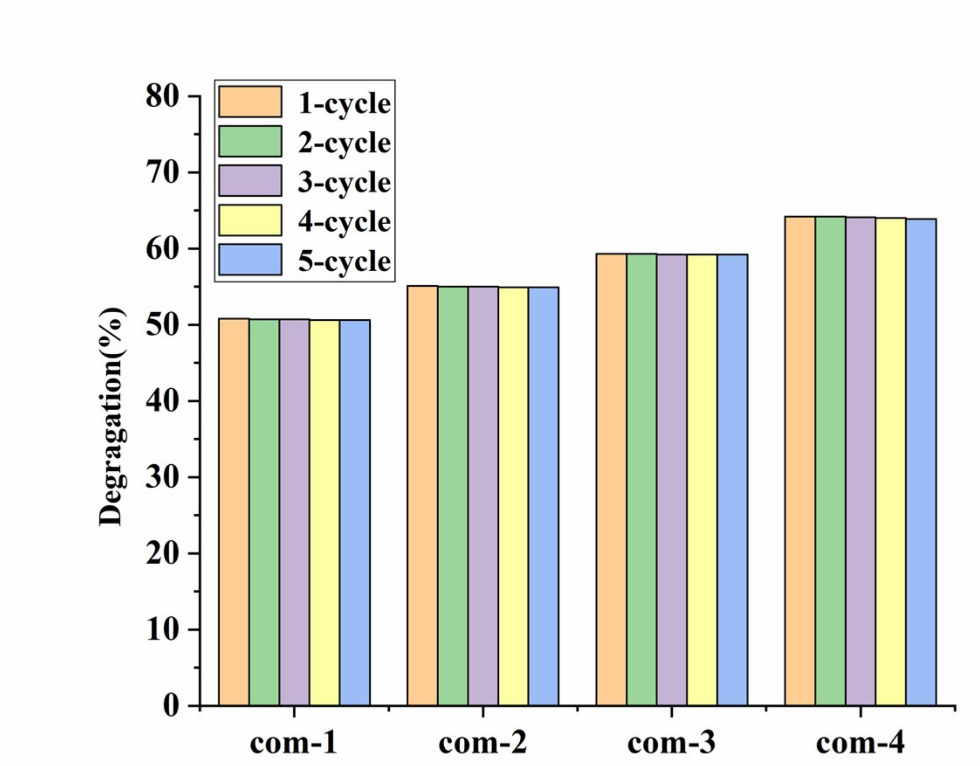

Fig. S16. Degradation rates of coordination polymers **1–4** as catalysts in cyclic test.

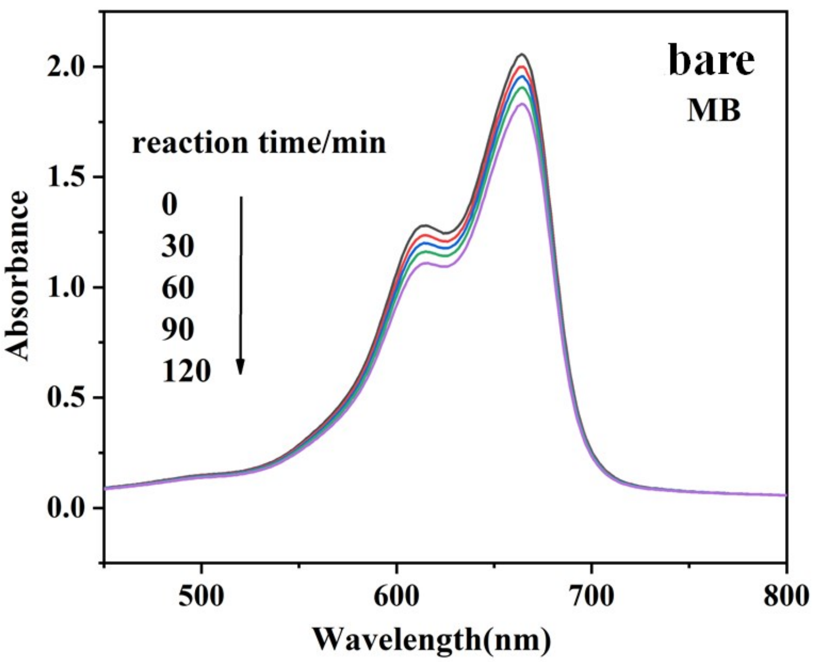

Fig. S17. Absorption spectra of the MB solution during the decomposition reaction under UV irradiation without the coordination polymers**.**

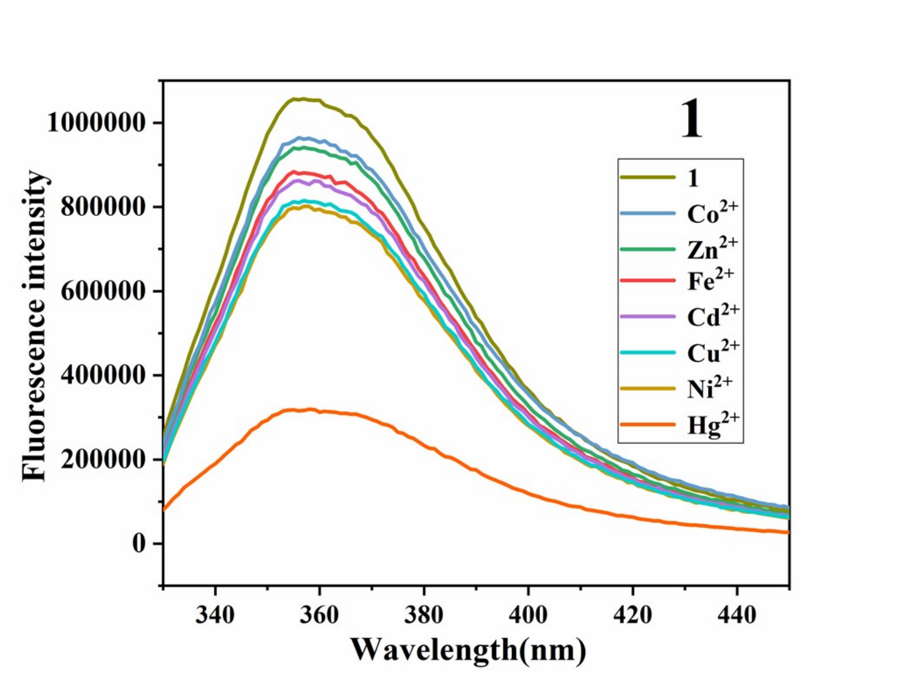

Fig. S18. Fluorescence intensity of coordination polymer **1** after adding other metal ions to the solution.

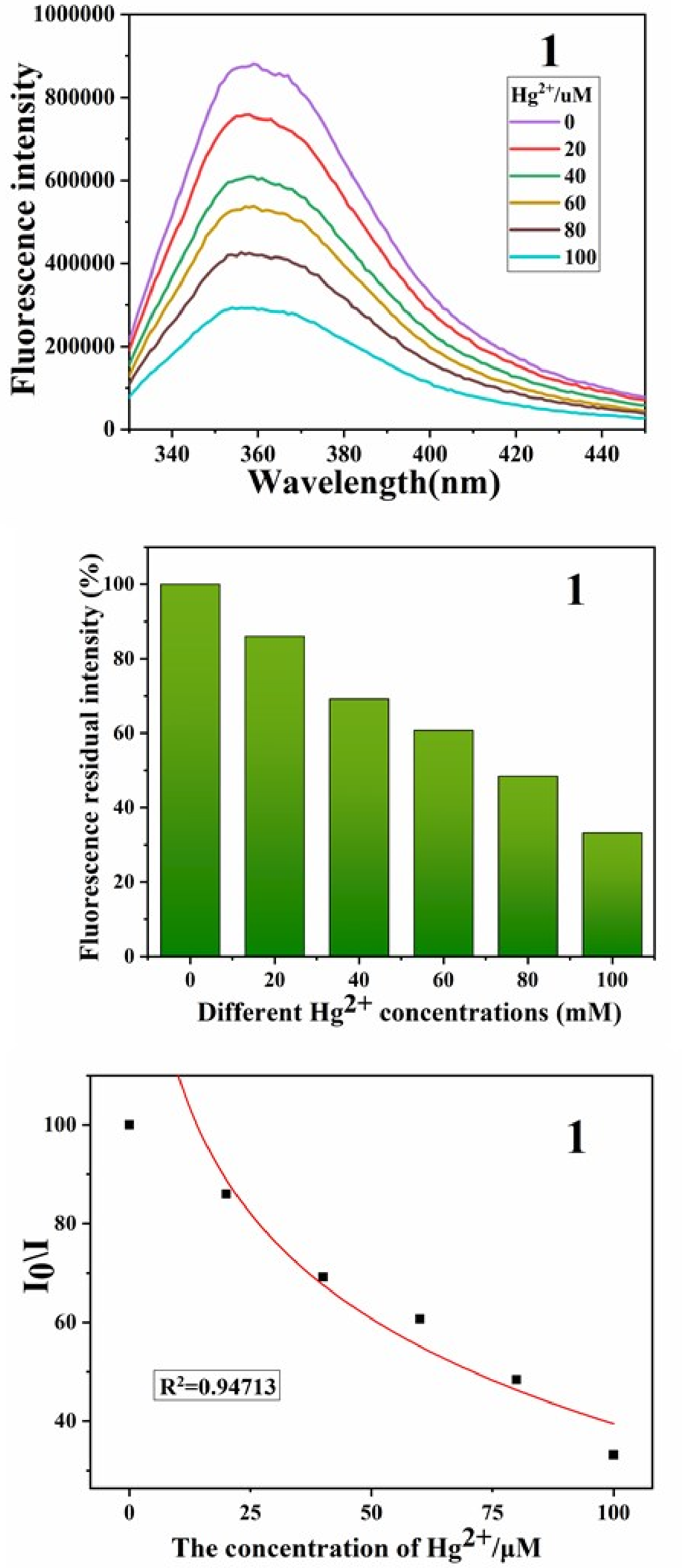

Fig. S19. (a) Fluorescence intensity of **1** suspension with the addition of different metal ions (excited at 310 nm); (b) bar chart of fluorescence intensity of **1** suspension with the addition of different metal ions ;(c) Curve fitting of fluorescence intensity changes.